Bima Journal of Science and Technology Vol. 2 No. 1 January, 2018 ISSN25366041

LITHO-MAGNETIC AND STRUCTURAL MAPPING FROM INTERPRETATION OF HIGH RESOLUTION AEROMAGNETIC DATA OVER NORTHERN BIDA BASIN AND ENVIRONS NORTH-CENTRAL NIGERIA

By

Jonathan Barka[1], Abubakar Yusuf[1] and Kamureyina Ezekiel[2]

[1]Department of Geology Gombe State University, Gombe State Nigeria.

[2]Department of Geology and Mining Adamawa State University, Adamawa State Nigeria.

Corresponding Authors E-mail: **joebarka@yahoo.com**

Abstract

Recently, the Nigerian Geological Survey Agency (NGSA) acquired high resolution airborne data over Nigeria and have commenced surface geological mapping in some parts of the country. This research becomes imperative taking into account time consumption and the risk associated with geological field mapping in recent time which includes difficulty in terrain coverage, abduction of field workers and insurgency in some part of the country. In this research an attempt was made to carry out litho-magnetic mapping and delineation of surface structures from interpretation of high resolution aeromagnetic data within northern Bida basin and environs. High resolution aeromagnetic data of the study area was subjected to regional residual separation, analytical signal, vertical derivative, tilt angle derivative, horizontal tilt derivative and upward continuation filters in the Oasis Montaj Version 7.0.1 Geo-software environment to enhance data for interpretation. Results from the total magnetic intensity (TMI) and residual data shows that magnetic intensity values range from 33,961.54 nT to 34,124.84 nT and -37.75nT/m to 124.08 nT/m respectively. Results of litho-magnetic mapping on the basis of magnetic susceptibilities helped in demarcating lithologies associated with Basement Complex and sedimentary terrains. Structures mapped in the study area are faults which trends in the NE-SW and NW-SE dominant directions and other minor direction are in the E-W. These results put together assisted in the preparation of a comprehensive litho-magnetic and structural map of the study area.

Keywords: High resolution aeromagnetic, litho- magnetic, magnetic susceptibility, northern Bida basin, structures

Introduction

In recent years, high resolution aeromagnetic data is playing a prominent role in earth sciences through revealing surface and subsurface information. Aeromagnetic maps generally show the variation in the magnetic field of the earth, therefore, mapping the variation of the crustal magnetic field mainly due to susceptibility of the crustal rocks has greatly assisted in geological mapping.

The magnetic susceptibility of most rock forming minerals is low, and the magnetism in rocks is as a result of the presence of magnetic minerals (Keary et al., 2002). The presence of different types

of magnetic minerals in various compositions in rock formation results in different rock formation having different magnetic susceptibility values. Basic igneous rocks are usually highly magnetic due to their relatively high magnetite content. The proportion of magnetite in igneous rocks tends to decrease with increasing acidity so that acid igneous rocks, although variable in their magnetic behaviour, are usually less magnetic than basic rocks (Keary et al., 2002). Metamorphic rocks are also variable in their magnetic character. If the partial pressure of oxygen is relatively low, magnetite becomes reabsorbed and the iron and oxygen are incorporated into other mineral phases as the grade of metamorphism increases. Relatively high oxygen partial pressure can, however, result in the formation of magnetite as an accessory mineral in metamorphic reactions (Milsom, 2003). However, sedimentary rocks are effectively non-magnetic unless they contain a significant amount of magnetite in the heavy mineral fraction. Where magnetic anomalies are observed over sediment covered areas the anomalies are generally caused by an underlying igneous or metamorphic basement, or by intrusions into the sediments (Milsom, 2003). In a nut shell Sediments and acid igneous rocks have small susceptibilities whereas basalts, dolerites, gabbros and serpentinites are usually strongly magnetic. Weathering generally reduces susceptibility because magnetite is oxidized to hematite, but some laterites are magnetic because of the presence of maghemite (Keary *et al*., 2002). Besides the presence of a magnetic mineral in a rock unit that would result in a magnetic anomaly, other common causes of magnetic anomalies include dykes, faulted, folded or truncated sills and lava flows, massive basic intrusions, metamorphic basement rocks and magnetite ore bodies.

Table 1 gives the magnetic susceptibility of some common rocks and minerals. In the year 2004-2009 the Nigerian Geological Survey Agency (NGSA) has acquired various high resolutions airborne data sets over Nigeria and has started mapping some parts of the country. However, surface geological mapping could be time consuming and will take many years before completion. Taking into cognisance time consumption and the risk associated with geological field mapping in recent time which include difficulty in terrain coverage, abduction of field workers, insurgency in some part of the nation and many other factors. This research attempt to carry out a litho-magnetic mapping and delineation of surface structures from interpretation of high resolution aeromagnetic data in an effort to conserve mapping time and minimize the risk factors associated with field work.

The study area is the northern sector of Bida Basin and environs located in the north-central part of Nigeria and falls within Longitudes $5^{0}00'$ to $7^{0}00'$E and Latitudes $8^{0}30'$ to $10^{0}30'$N. Major towns within the study area include: Kontagora, Zungeru, Bida, Lapai, Minna, Wushishi, Enagi, Sapkpe, Mokwa Pategi, Agena Agiea (Fig.1). The geology of northern Bida basin and environs consists of the Basement Complex rock, flanking a

central sedimentary basin. Lithologies in this basin consist of Bida Sandstone, Sakpe Iron stone, Enagi Siltstone and Batati Iron stone Formations (Obaje, 2009; Nwajide, 2013).

Table 1: Magnetic Susceptibility Values of some common Rocks and Minerals [Bullock and Isle (1994); Fallon and Backo (1994); Lowrie (1997)]

S/No. (SI)	Rocks/Minerals	Susceptibility Range
1.	Sandstone	0 - 20
2.	Shale	0.01 - 15
3.	Schist	0.3 - 3
4.	Gneiss	0.1 - 25
5.	Slate	0 - 35
6.	Granite	0 - 50
7.	Basalt	0.2 - 175
8.	Gabbro	1 - 90
9.	Quartz	-0.01 – 0.02
10.	Calcite	-0.0011 – 0.01
11.	Haematite	0.5 - 35
12.	Magnetite	1200 - 19200

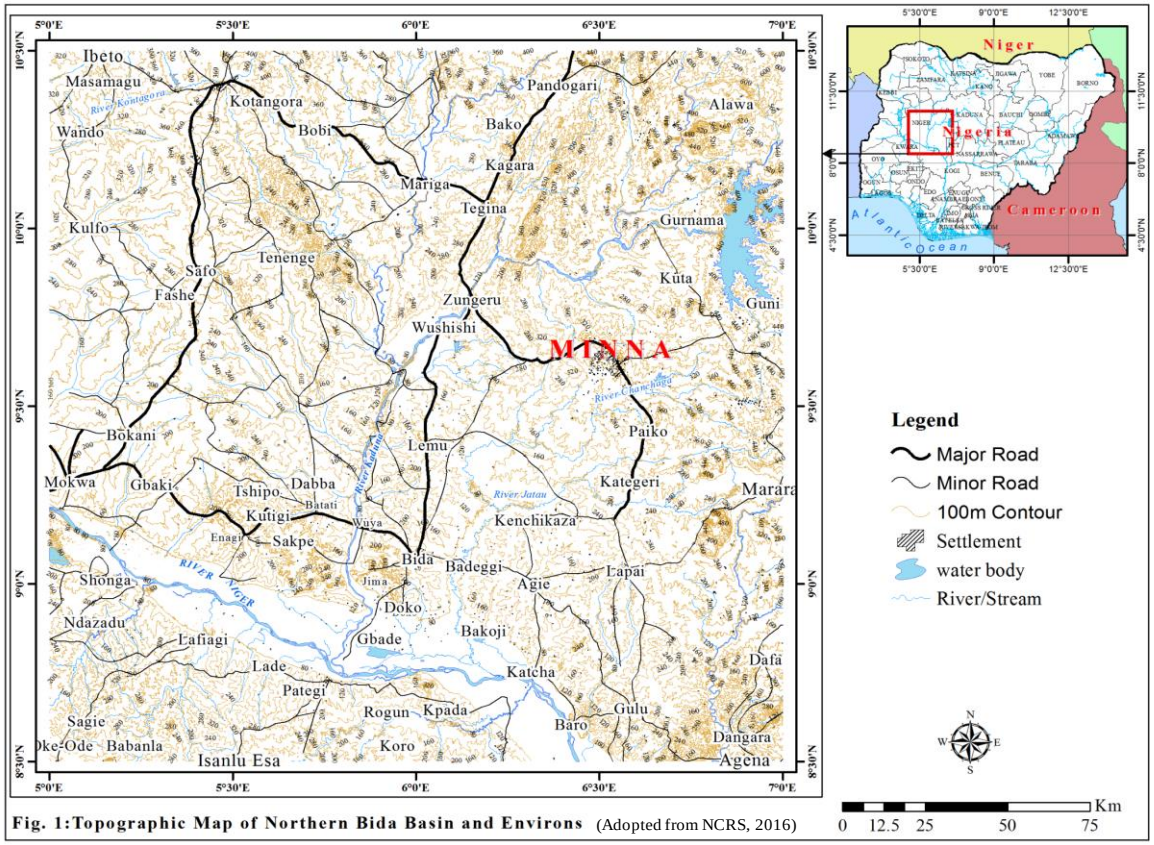

Fig. 1:Topographic Map of Northern Bida Basin and Environs (Adopted from NCRS, 2016)

Methodology

Materials

Sixteen (16) high resolution aeromagnetic data each on a scale of 1:100,000 which were provided in both grid and data based format were used for this work. The data was acquired by Fugro Airborne Survey Ltd. in the year 2004-2009 using 3X Scintrex CS3 Cesium Vapour Magnetometer with the following flight parameters: flight line spacing was 500 metres, terrain clearance was 80 metres, flight direction was in the NW-SE, tie line spacing was 2 kilometres and tie line direction was in the NE-SW direction. Additional materials used include Oasis Montaj Version 7.0.1 and Surfer 11 softwares.

Methods

Litho-magnetic and Structural Mapping

To enhance data for interpretation, this research work utilises MAGMAP filters within the Oasis Montaj Version 7.0.1 environment such as regional residual separation, analytical signal, vertical derivative and tilt angle derivatives:

Regional Residual Separation

The residual magnetic field data was separated from the regional magnetic field data using the regional residual separation method. Residual magnetic field data was obtained as the deviations of the fitted plane surface from the total magnetic intensity. This method unlike the other methods does not change the amplitude of the shallow features or change the shape

apart from the removal of the long wave lengths. The regional residual separation filter was applied to the total magnetic intensity field (TMI).

Analytical Signal

Nabighian (1984), developed the concept of analytical signal of magnetic anomalies which was calculated by taking the square root of the sum of squares of the data derivatives in the x, y, and z directions of magnetic field as follows:

$$|A(x,y)| = \mathbf{(}(dT/dx)^2+ (dT/dy)^2+ (dT/dz)^2\mathbf{)}^{1/2} \quad \ldots\ldots\ldots\ldots\ldots\ldots \quad (1)$$

The resulting shape of the analytic signal which was centred on the causative body is independent of the orientation of the magnetization of the source. This filter is advantageous because it is immune to IGRF field direction, that is, you do not need to precede this calculation with a reduction to equator filter, however in this work the analytical signal was directly applied on the TMI.

a) Vertical Derivative:

Computation of vertical derivative to an aeromagnetic data is equivalent to observing the vertical gradient directly with a magnetic gradiometer and has the same advantage, as enhancing shallow sources, suppressing deeper ones, and giving better resolution of closely-spaced sources. Second vertical derivatives were computed using convolution filter and laplace's equation related by the following equation:

$$\nabla^2 f = 0 \text{ so,} \quad (2)$$

$$\frac{\partial^2 f}{\partial z^2} = -\left(\frac{\partial^2 f}{\partial x^2} + \frac{\partial^2 f}{\partial y^2}\right) \quad (3)$$

Once the Fourier filtering techniques becomes available, the n^{th} order vertical derivative is computed using the following relationship:

$$F\left(\frac{\partial^n f}{\partial z^n}\right) = k^n .F(f) \quad (4)$$

Where F is the Fourier representation of the field and k is the wave number or frequency.

Vertical derivative filter was applied to the data to detect the edge of shallow features on the magnetic grid and this filter was able to clearly bring out the geological boundaries and their discontinuities on the map.

b) Tilt Angle Derivative

The tilt derivative method which is the ratio of first vertical derivative to the horizontal gradient enhances subtle and major features evenly. The tilt derivative and its total horizontal derivative are useful for mapping shallow basement structures and mineral exploration targets. Miller & Singh, (1994), and Salem et al., (2007, 2008) defined the tilt derivative as:

$$\theta = \tan^{-1}\left[\frac{\partial M}{\partial z} \Big/ \frac{\partial M}{\partial h}\right] \quad (5)$$

Barka *et al*., 2018

$$\text{where } \frac{\partial M}{\partial h} = \sqrt{\left(\frac{\partial M}{\partial x}\right)^2 + \left(\frac{\partial M}{\partial y}\right)^2} \quad (6)$$

and ƏM/Əx, ƏM/Əy, ƏM/Əz are derivatives of magnetic field M in the x, y, z directions.

$$\frac{\partial M}{\partial z} = 2KFc \sin d \frac{h\cos(2I-d-90) - z\sin(2I-d-90)}{h^2 + z_c{}^2} \quad (7)$$

$$\frac{\partial M}{\partial h} = 2KFc \sin d \frac{z_c\cos(2I-d-90) - h\sin(2I-d-90)}{h^2 + z_c{}^2} \quad (8)$$

Where K is the susceptibility contrast at the contact, F is the magnitude of the magnetic field, c = 1-cos^2 *i* sin^2 A, A is the angle between the positive h –axis and the magnetic north, *i* is the ambient field inclination, tan I = tan i/cos A, d is the dip (measured from the positive h-axis) and all trigonometric quantities are in degree.

And for vertical contacts:

$$\frac{\partial M}{\partial z} = 2KFc \frac{h}{h^2 + z_c{}^2} \quad (9)$$

$$\frac{\partial M}{\partial h} = 2KFc \frac{z_c}{h^2 + z_c{}^2} \quad (10)$$

Substituting equation 12 and 13 into equation 8 gives:

$$\theta = \tan^{-1}[h / z_c] \quad (11)$$

In this work the tilt angle filter was applied to residual data this brings out the basement fractures and lineaments clearly which was used as a guide in the preparation of a comprehensive litho-structural map of the area.

Results and Discussion

Results

To obtain the actual total magnetic intensity (TMI) values on figure 2, 33,500 nT was added to each magnetic intensity values therefore, from (Fig.2) the aeromagnetic intensities range from 33,961.54 nT to 34,124.84 nT. This range of magnetic intensities implies that the study area is characterised by high to low frequency of magnetic intensities. The total magnetic intensity (TMI) map (Fig.2) reveals that areas of high magnetic intensity values represented by red to magenta colours are found around Bakoji, Katcha, Wushishi, Tshipo, Iasnlu Esa, and Kategeri. The low magnetic intensity values represented by deep blue colour, occurs in areas around Pandogeri, Dobi, Gurnama. Kuta, Ibeto, Masagamu, Wando, Tenenge, Safo, Zungeru. Agie Jima Doka, and Age. Whereas, the remaining part of the study area comprising of Enagi, Gulu, Lemu, Paiko, Bakoni, Fashe, Minna and Alawa areas exhibit modest magnetic intensities. The residual map over the study area (Fig.3) shows attributes of positive and negative anomalies scattered in different parts of the map.

Using two set of filters within the Oasis Montaj environment, analytical signal (AS) and first vertical derivative (FVD) the high resolution aeromagnetic data covering the study area was analysed to enhance data for litho-magnetic demarcation. Figure 4 is a map of the analytical signal of TMI, from figure 4 six (6) different anomalous zones representing different lithologic discontinuities were identified. Anomaly labelled **S** is seen to occupy the central region of the study area, the anomaly has low magnetic susceptibility of the range 0.01 nT/m to 0.04 nT/m (deep blue to orange colour). The second anomalous zone labelled **MS** also exhibits low magnetic anomaly of 0.01 nT/m (deep blue colour) were seen to occur in the north-eastern part of the area. Anomalies labelled **MV** are of moderate magnetic susceptibility and were seen to

occupy the north-western, north, north-eastern and south-western parts of the study area. They are obviously noticed on the map by deep yellow colour with deep blue spots in their centre depicting a decrease of magnetic susceptibility towards the centre and have a susceptibility range of 0.04 nT/m to 0.06 nT/m. Anomalies labelled **IG** were characterized by a circular to near circular shapes exhibiting moderate high anomaly of the range 0.06 nT/m to 0.08 nT/m. These anomalies which were represented by light red colours with magenta colour spots in their centre indicate anomaly increase towards the centre.

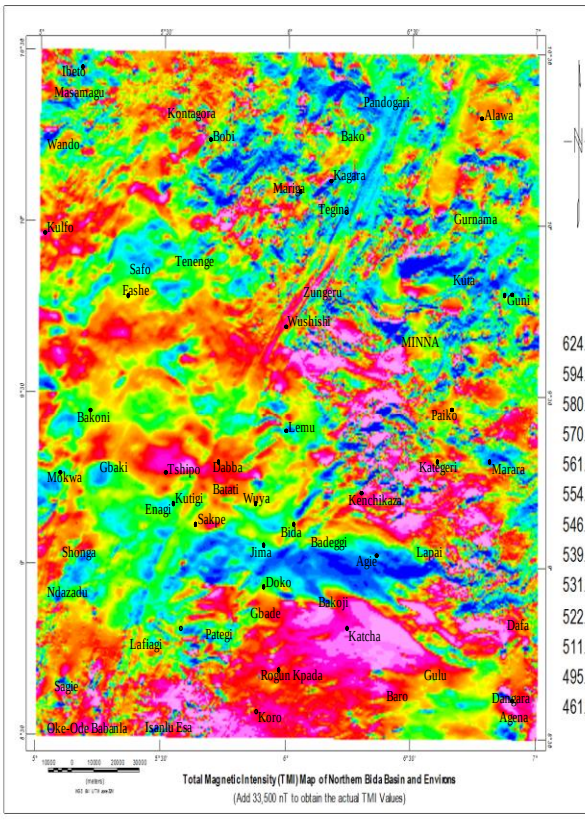

Fig. 2: Total Magnetic Intensity (TMI) Map of Northern Bida Basin and Environs

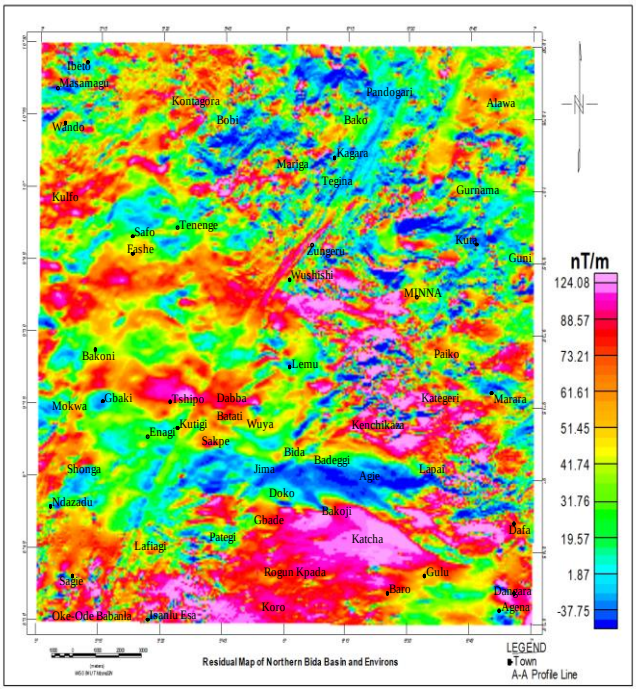

Fig. 3: Residual Map of Northern Bida Basin and Environs

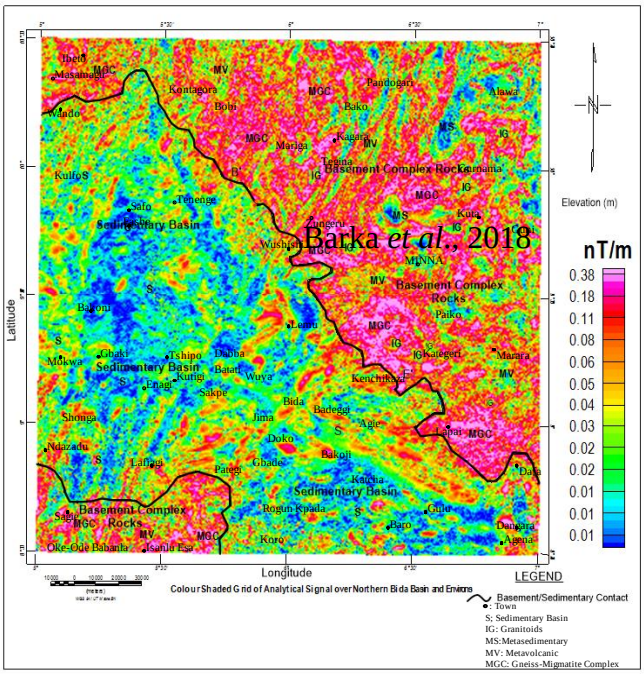

Fig.4: Analytical Signal Map of Northern Bida Basin and Environs

The highest magnetic susceptibility of the range of 0.11 nT/m to 0.38 nT/m (deep red to magenta colour), labelled **MGC** is the dominant lithology occupying the south-western, north-western, north-eastern and even the eastern part of the study area.

Vertical derivatives tend to sharpen the edges of anomalies and enhance shallow features hence it was used to delineate high frequency features more clearly where they are shadowed by low frequency features. A colour-shaded scale was applied to the first vertical derivatives data and this has aided in the demarcation of the different lithologic boundaries within the sedimentary basin as shown in figure 5. Both positive and negative anomalous zones within the sedimentary basin were depicted from figure 5. Anomaly labelled **A** has a positive magnetic amplitude of 0 nT to 10 nT, the second anomaly within the area demarcated as the sedimentary basin labelled anomaly **B** with magnetic amplitude of 10 nT to 20 nT occurs in the northwest of anomaly A. Anomaly labelled **C** extending from the northwest to the southeast records a positive amplitude of 20 to 30 nT/m and negative anomaly amplitude of -40 nT to -10 nT/m. The highest and positive anomalous zone labelled **D** with amplitude of 40 nT/m occurs at the extreme south-eastern corner of the map.

The enhancement of magnetic anomalies associated with faults and other structural discontinuities was achieved by the application of tilt angle derivative filter. From figures 6 and 7 the anomaly range of tilt derivative map and its horizontal derivatives (HD_TDR) are -1.23 nT/m to 1.39 nT/m and 0.001nT/m to 0.009 nT/m respectively. Structural trends from these maps are not discernible probably because they are shadowed by low frequency anomalies. By subjecting the tilt derivative and its horizontal derivative to an upward continuation to 1 km to filter out low frequency anomalies and then generating their corresponding shaded relief maps at a sun angle of 60^0 structural lineaments can now be identified. Figure 8 shows structures superimposed on the shaded relief map of tilt derivative, a major structure labelled **F1** trending in the NE-SW direction cutting across the study area is delineated. Other structures identified in figure 8 include those labelled as **F** which trends dominantly in the NW-SE, NE-SW and E-W as minor trends, and those labelled **SF**. Figure 9.

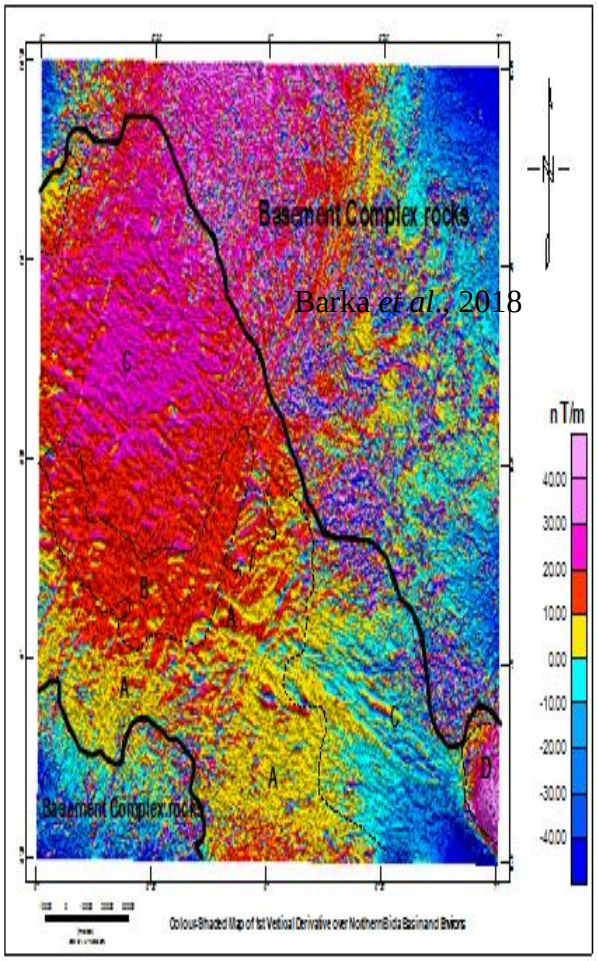

Fig. 5: Colour Shaded Map of 1st Vertical Derivative over Northern Bida Basin and Environs

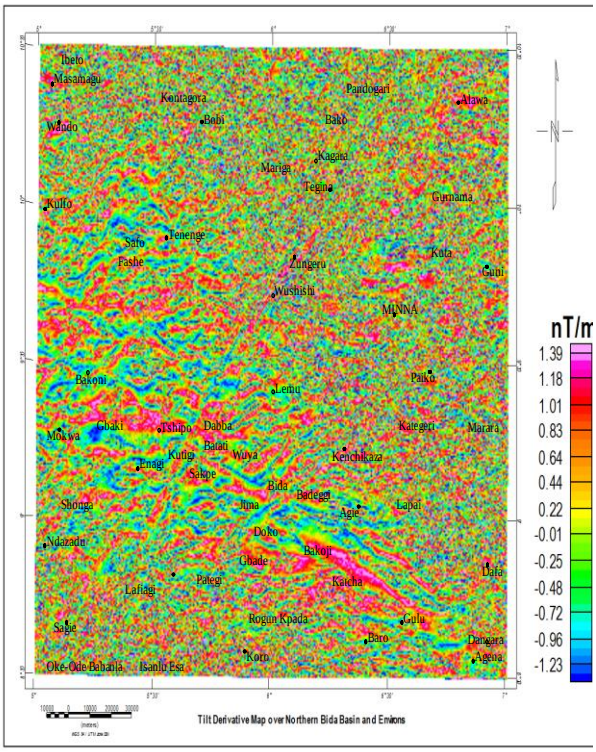

Fig. 6: Tilt Derivative Map draped on the Study Area

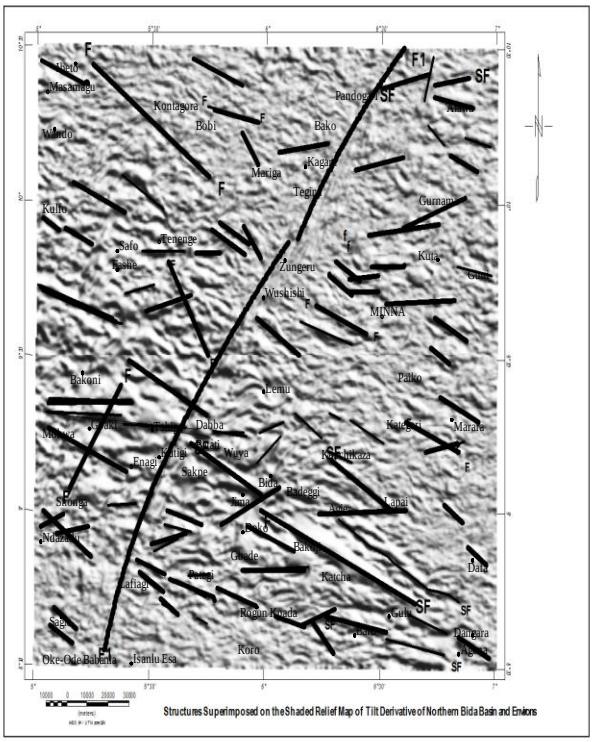

Fig. 8: Structures Superimposed on the Shaded Relief Map of Tilt Derivative

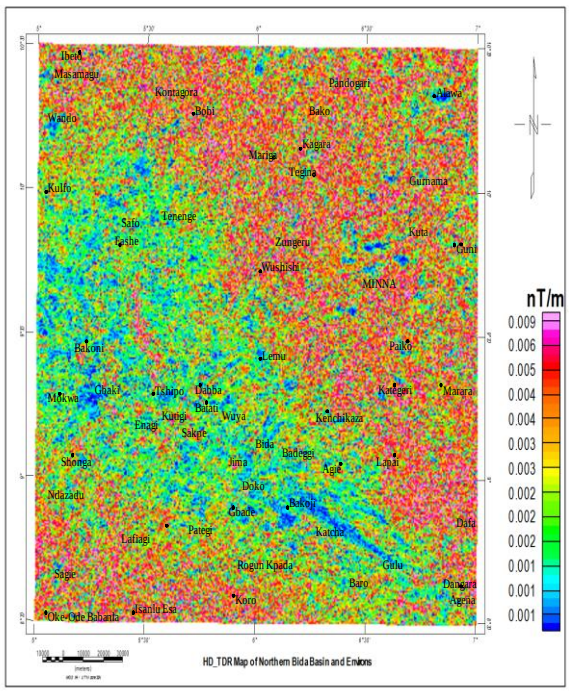

Fig. 7: Horizontal Derivative of TDR Map draped on the Study Area

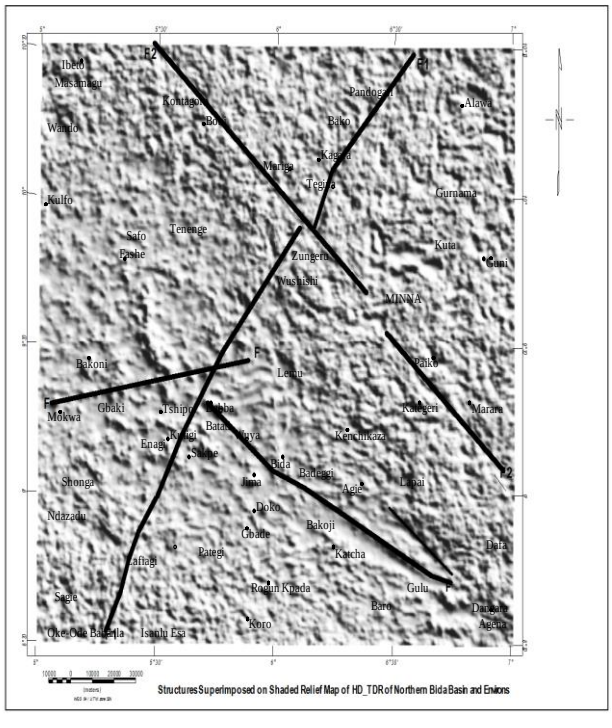

Fig. 9: Structures Superimposed on the Shaded Relief Map of HD_TDR

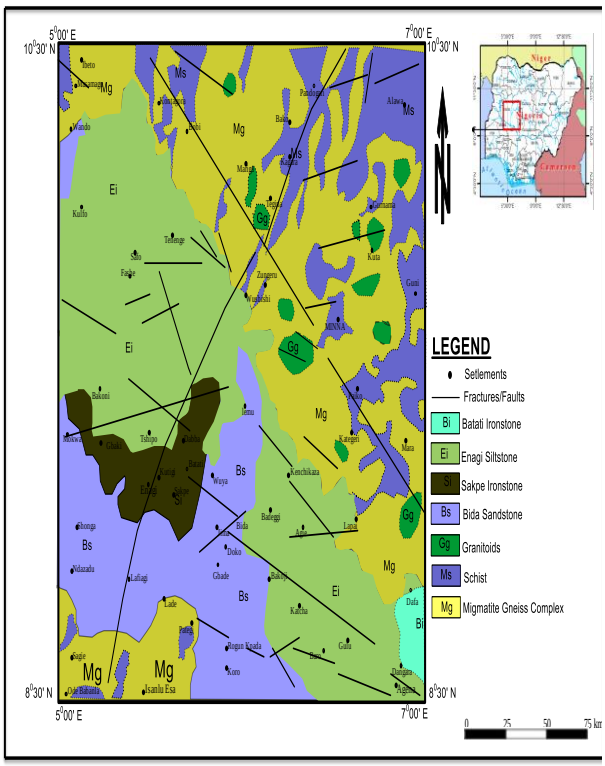

Fig. 10: Litho-magnetic and Structural Map of Northern Bida Basin and Environs

Further revealed other structures, example is a major structure labelled **F2** which trends in the NW-SE off–setting **F1.** Other structural trends labelled as **F** were also identified (Fig. 9). Combination of results from analytical signal (AS), first vertical derivative, (FVD) Tilt angle/Horizontal derivatives (HD_TDR) was used in the generation of the litho-magnetic and structural map of the study area (Fig.10).

Discussion

The magnetic field of northern Bida Basin and environs as revealed from form the total magnetic intensity map (Fig.2) is a contribution of short, medium and long wavelength anomalies. The residual map (Fig.3) exhibits both positive and negative magnetic anomalies. The positive anomalies recorded within Bida basin and environs have a value range of 70.06 to 124.08 nT/m. This positive anomaly is an indication that the lithologies within these areas contain in them some magnetic grains hence the positive anomalies (Milsom, 2003). A negative anomaly of the range -37.75 to - 4.55 nT/m is an indication of the absence of ferro- or ferri-magnetic substances in the lithologies within these areas (Milsom, 2003).

Result of the analytical signal over northern Bida basin and environs (Fig.4) shows a clear demarcation between the basement/sedimentary contacts and to some extend the different Basement Complex lithologic boundaries. In the interpretation of these anomalies the geological map of the study area was also taken into cognisance. From (Fig.4), different lithologic discontinuities labelled S, MS, MV, IG, and MGC was mapped on the basis of magnetic susceptibility contrast and these were compared with that-obtained from table 1 for interpretation purposes. From analytical signal map, the formation labelled **S** recorded the lowest magnetic intensity and low magnetic intensity is generally associated with sediments (Milsom, 2003). This suggests that the lithology labelled **S** which is indicated by deep blue colour is made up of sedimentary rocks. Within areas demarcated as Basement Complex terrain lithologies labelled as **MS** also records low magnetic anomaly and was depicted by deep blue colour this suggest that the lithology could have its source from sediments and this was interpreted to be meta-sedimentary schist belt. The average magnetic signatures registered in some parts within the Basement Complex terrain labelled as **MV** suggest that, these

lithologies are meta-volcanic schist belts. Anomalies labelled **IG** and **MGC** yielded the highest magnetic anomalies and were interpreted as igneous rocks and the Undifferentiated Migmatite-Gneiss-Complex respectively.

The first vertical derivative map has helped in defining the different lithologies associated with the sedimentary basin. From the colour shaded map of 1st vertical derivative (Fig.5) both positive and negative anomalies exist within area demarcated as the sedimentary basin in northern Bida basin and are labelled A, B, C, and D. Anomaly **A** with positive anomaly range of 0 to < 10 nT/m was interpreted as Bida Sandstone Formation, according to literature this formation consist dominantly of sandstone other lithologies include breccias, argillaceous rock and occasional bands of ferruginized dark-brown sandstone (Obaje, 2009; obaje *et al*., 2013; Nwajide, 2013). The ferruginous sand stone could have contributed to the low positive anomaly observed in this formation. Anomaly **B** records a magnetic anomaly of 10-20 nT/m and was interpreted as Sakpe Ironstone Formation. This formation consists dominantly of oolitic and pisolitic ironstone with occasional claystone at the base (Obaje et al., 2013). This is the possible reason why this formation is associated with high positive magnetic anomaly. Anomaly C exhibits both positive of 10-30 nT/m and negative anomaly ranging from -40 to -10 nT/m. The positive high anomaly C observed north of anomaly B could have resulted from chemical weathering and precipitation of iron from the nearby iron rich Sakpe Formation and the negative anomaly is an attribute of thick pile of sedimentary rock absence of magnetic grains. This anomaly was interpreted to be associated with Enagi siltstone Formation which consists mainly of siltstone and other subsidiary lithologies include sandstone-siltstone admixture with massive claystone and shale. The highest and positive anomaly of 40 nT/m labelled **D** was interpreted as Batati Ironstone Formation. Its lithology consists of argillaceous, oolitic ironstone with ferruginous siltstone and shaly bed intercalation. Obaje *et al*., (2013) showed that this formation occupy a rifted sink (graben) hence, areas covered by this formation presents the thickest sedimentary pile and this could be the possible reason for the circular shaped high positive anomaly.

Tilt derivative and its horizontal derivative filters were used to analyse the structural disposition within the study area. Structures superimposed on shaded relief of tilt derivative and HD_TDR (Figs.8 and 9) shows major structural feature labelled **F1** running from Ode Babanla through Lafiagi, Enagi, Kutigi, Wushishi Tegina and Pandogari trending in the NE-SW direction was interpreted to be a major fault cutting across the northern Bida basin and environs. Other structural features identified trending in the same NE-SW direction (labelled **F**) interpreted to be faults and fractures are those recognized in areas like Mokwa, Gurrnana, Gbaki, Shonga and Jima. Additional structures interpreted as fault and fractures are those trending in the NW-SE direction and occur in areas like Ibeto, Kontago, Mariga,

Gbaki, Bakoji, Wuya etc. Other structures labelled **SF** interpreted as strike-slip faults were also identified. The strike-slip fault as observed in areas around Alawa, Bida and Rogun Kpada are major strike slip faults and are seen to exhibit a general dextral sense of movement. From the shaded relief map of HD_TDR, major structural feature trending in NW-SE direction and traversing through Marara, Paiko, Mariga, Bobi and Kontagora was identified and labelled as **F2.** This feature, which was also interpreted as a major fault was seen to off-set **F1** at Zungeru and this resulted to a strike-slip faulting of **F1** with a dextral sense of movement. **F2** is believed to be the extension of a major sinistral strike slip fault reported by Whiteman (1982) as Boko transform fault. Other minor trends of structures interpreted as fault and fractures identified on both maps of structures superimposed on shaded relief of tilt derivative and HD_TDR are in the E-W direction. From the structural trends of NE-SW, NW-SE and E-W directions, the area can be said to have been effected by three major tectonic episodes.

Conclusion

This research work has demonstrated the usefulness of high resolution eromagnetic data interpretation in mapping different lithologies and structures associated with both Basement Complex rocks and the sedimentary basin on the basis of magnetic susceptibility. Lithologies associated with the Basement Complex environment in the study area example migmatite gneiss, schist and igneous intrusions were mapped. Also those formations associated with the sedimentary basin (Bida Sandstone, Sakpe Ironstone, Enagi Siltstone and Batati Ironstone Formations) were mapped on the basis of magnetic susceptibility. Structures such as fault and fractures were also mapped. In respect to this, a litho-magnetic/structural map of the study area was produced.

Acknowledgement

The authors acknowledged with profound gratitude Tertiary Education Trust Fund special intervention and Gombe State University for giving grant to one of the authors for his doctorate research work. We also acknowledged all authors whose work(s) were cited in this research work.

References

Bullock and Isles (1994). Magnetic Susceptibility of common Rocks. Amazon publishers. 33p.

Fallon and Backo (1994). Magnetic Minerals and and their Magnetic Susceptibility. World Geosciences Vol.2.pp 12-16.

Kearey, P., Brooks, M. and Hill. I. (2002). An introduction to Geophysical Exploration (3rd Edit), Published by Balckwell Science Ltd. 281p.

Lowrie, W. (1997). Fundamentals of Geophysics. Published by Cambridge University Press. 353p.

Miller, H.G. and Singh, V. (1994). Potential field tilt; a new concept for location of potential field sources. Journal of Applied Geophysics.,Vol.32, pp.213-217.

Milsom, J. (2003). Field Geophysics (3rd Edit). Published by John Wiley and Sons Ltd. 232p.

Nabighian, M.N. (1984). Toward a Three-dimensional Automatic Interpretation of Potential Field Data via Hilbert transforms – Fundamental Relations. Geophysics, Vol.49, pp.780-786.

National Centre for Remote Sensing Jos (2016). Tophographic Map of Northern Bida Basin and Environs

Nwajide, C.S. (2013). Geology of Nigeria's Sedimentary Basins. Published by CSS Bookshop Limited. 565p.

Obaje, N.G. (2009). Geology and Mineral Resources of Nigeria. Publishes by Springer, Dordrecht Heidelberg London New York. 218p.

Obaje, N. G., Balogu, D.O., Idris-Nda, A., Goro. I.A., Ibrahim, S.I., Musa, M.K.., Dantata, S.H., Yusuf, I., Mamud-Dadi, N. and Kolo, A.I. (2013). Preliminary Integrated Hydrocarbon Prospectivity Evaluation of Bida Basin in Northcentral Nigeria. Petroleum Technology Development Journal. Vol. 3(2) pp.36–65.

Salem, A., Williams, S., Fairhead, D., Smith, R. and Ravat, D. (2008). Interpretation of Magnetic data using Tilt-angle derivatives. *Geophysics, 73*(1), pp1-10.

Whiteman, A. J. (1982). Nigeria, its Petroleum Geology, Resources and Potentials. Graham and Trotman, London. 394p.